DYNAMIC POST-ANALYSIS OF A FEED WATER PIPE BREAK AT THE LOVIISA NUCLEAR POWER PLANT

Arja Saarenheimo

Lauri Eerikäinen

Rauli Keskinen

SUMMARY

A dynamic post-analysis is presented for a sudden pipe break which occurred in the main feed water system of the VVER 440 type PWR plant Loviisa 2 on February 25, 1993. A thermal hydraulic code TMOC, based on the method of characteristics, is first used to determine the induced rapid two phase fluid transients. The resulting pressure and momentum flux histories are then applied as an excitation in a nonlinear structural dynamic analysis which makes use of the general purpose finite element code ABAQUS. The permanent relative displacement of the broken pipe ends is finally compared with the value observed after the event. An underestimate of some 30% may for the most part be attributed to scant experimental data and uncertainties in boundary conditions. Assumptions regarding impact against a nearby beam structure and the dynamic stress-strain curve of the ferritic pipe material strongly affect this comparison.

INTRODUCTION

Apart from the widening applications of the leak-before-break criterion to nuclear piping systems /1/, the postulated double-ended guillotine break (DEGB) still has a marked

position in the regulatory policies of many countries using nuclear energy. Among recent licencing activities are numerous DEGB reanalyses of primary circuit piping, undertaken to redesign the sump structures. The need for such remedies stems from the pipe break induced thermal insulation debris, which causes a potential for clogging of the emergency core cooling system sumps.

DEGB analysis methodologies and applications to pipe whip restraint design were developed in the mid-1970s /2/. Owing to enormous advances in the disciplines of two phase thermal hydraulic and elastic-plastic finite element analysis during the past two decades, much more powerful general purpose computer codes are now commercially available. With due consideration to fluid dynamic excitation and jet impingement dynamics, such codes enable numerical prediction of the entire system response and identification of targets and damage chains resulting from extensive pipe whip phenomena. Unprotected safety related components in the vicinity of high energy piping, not qualifying for leak-before-break, provide one application area for this type of analysis.

This paper deals with a dynamic post-analysis of a real DEGB which occurred in the main feed water system of the VVER 440 type PWR plant Loviisa 2 on February 25, 1993. The incident was directly caused by erosion-corrosion and has been reported elsewhere /3/. As shown in Fig. 1, the break occurred at a dramatically thinned welded connection joining an expansion collar and a flange downstream of a check valve which was located on the discharge side of one of the five parallel main feed water pumps. With the plant operating at full power, a start-up of the pump was being initiated after an overhaul made for cleaning a strainer on the suction side. The eye-witnessing pump maintenance personnel then observed a leak on one side of the flange which gradually extended around the circumference until a complete pipe break occurred. No personal injuries were sustained and the leak was safely isolated 9 minutes after the break.

The pipe whip developed a permanent axial displacement of 560 mm in the vertical pipeline and made the next horizontal pipe portion impact against a nearby beam structure.
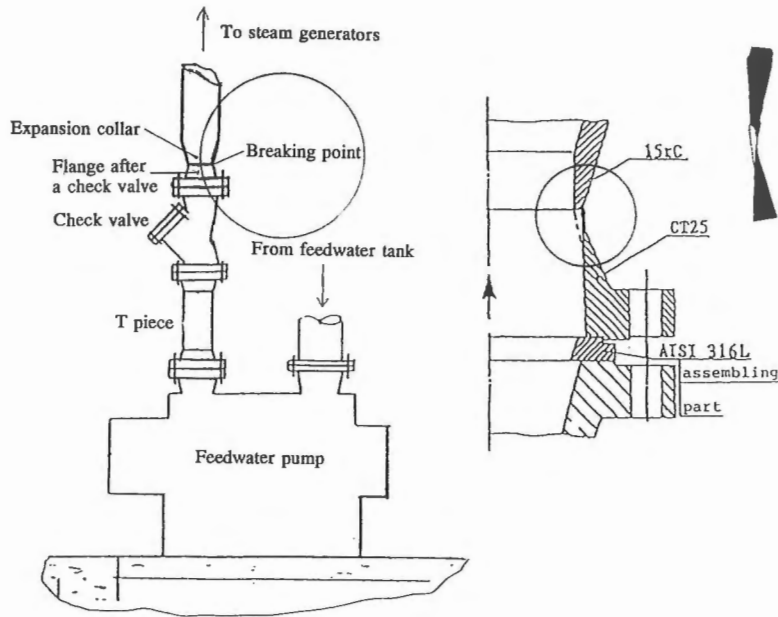
Fig. 1. Location of the pipe break.

No measured process data are available on the fluid transients during the incident; a thermal hydraulic code TMOC, based on the method of characteristics, was therefore used to determine them theoretically. The structural dynamic response was obtained using the general purpose finite element code ABAQUS. Integration of the decaying response over the first few cycles provided an estimate for the permanent deflection, which was compared with the observed value.

THERMAL HYDRAULIC MODELLING

The thermal hydraulic analyses were carried out using the computer code TMOC /4,5/ developed at the Technical Research Centre of Finland (VTT) for calculation of fast transients in a two phase flow. Based on the method of characteristics, the code handles abruptly changing phenomena, such as travelling waves in a network, physically correctly without unrealistic damping. To enable accurate description of phase changes,

43

the code includes several models for flashing and condensation rates as a function of the steam void fraction and other governing variables. These models are of great physical importance in case of pipe breaks and similar fast transients where a rarefaction wave enters pipes containing pure liquid water. The code has been benchmarked against several experimental tests and standard problems as well as interesting cases from practice.

The computational models of TMOC are defined as a piping network, filled with water and vapour, and consisting of pipes, reservoirs, throttlings and various types of valves and pumps. The pipes may be further subdivided into shorter sections. The physical quantities are solved at nodes which are located at either end of the pipe sections. A computational model of 13 pipes and 115 pipe sections as shown in the schema of Fig. 2, was used for the present analysis. It consists of a broken feed water discharge line of length 25 m, inner diameter 289 mm and wall thickness 18 mm, which leads to a T-connection with the main feed water line. The discharge line has two valves, fully open

Fig. 2. Feed water piping system to be analysed.

during the incident, and a highly throttling flow meter with orifice of diameter 222 mm. Two physically different parts constitute the model for the main feed water line. The first is a straight pipe of length 15 m. The second part, of length 19.2 m and initial temperature 226°C describes the preheaters and following portion of piping which ends at an infinite reservoir, representing a steam generator. The enthalpy of this reservoir corresponds to a temperature of 242.6° C at pressure 4.69 MPa. All other parts of the piping network are initially subjected to temperature 164° C and internal pressure of ca. 7.0 MPa. For further considerations it is worth noting that the saturation pressures at temperatures 164°C and 226° C are 0.68 MPa and 2.6 MPa, respectively.

The break occurred at node 1 of the flow model where the expansion collar has a minimum inner diameter of 205 mm, well below that of the discharge line. The breaking hypothesis of Malnes /4/ with the Mach number of 0.99 was used to model reaching critical flow conditions at the broken pipe end. No measured process data is available regarding the development of the break; hence its duration was assumed to be 15 ms. Earlier pre-calculations indicate that the exact duration is not very essential as it affects the rate of pressure decrease at the start of discharge only. The flashing (evaporation) model constitutes an other important boundary condition for the analyses. Based on the verification calculations, the Houdayer correlation /4/ with constants 0.003 and 4.0 and correction factor 4.2 was employed in the final analysis.

FLUID DYNAMIC EXCITATION

Using the theorem of conservation of momentum, it may be shown that the fluid dynamic excitation of the piping originates from the cross-sectional pressure and momentum flux resultants and their differentials at the discontinuities which include the broken pipe end, pipe bends, T-connections, changes of diameter and other minor losses /6/. Within each straight portion, these resultants are in dynamic equilibrium with the forces due to temporal accelerations and density changes of the contained fluid domain. While integration of the latter would yield the excitation as overall forces applied on

each straight pipe, the pressure and momentum flux formulation is preferred here as it readily produces a load distribution which physically excites the piping. However, care must be exercised in finite element implementation based on open-ended elements under internal pressure; whenever the fictitious pipe wall becomes incompatible at the nodal points (discontinuity in diameter, intersecting straight pipes etc), respective pressure and momentum flux resultants must be added or removed manually.

Excitation of the discharge line is presented in Fig. 3 in terms of the algebraic sum of the pressure and momentum flux (equivalent pressure) values obtained from thermal hydraulic analysis for five different nodes, defined in Fig. 2. Immediately after the break, the equivalent pressure is seen to decrease rapidly and to fall for a short time below the saturation pressure. The actual pressure falls even further at the break point owing to the critical mass flow rate. Vapour bubbles then start to form, returning the pressure to the saturated state in the piping section preceding the flow meter. The equivalent pressure reaches a value of ca. 1.0 MPa. Downstream of the flow meter, the
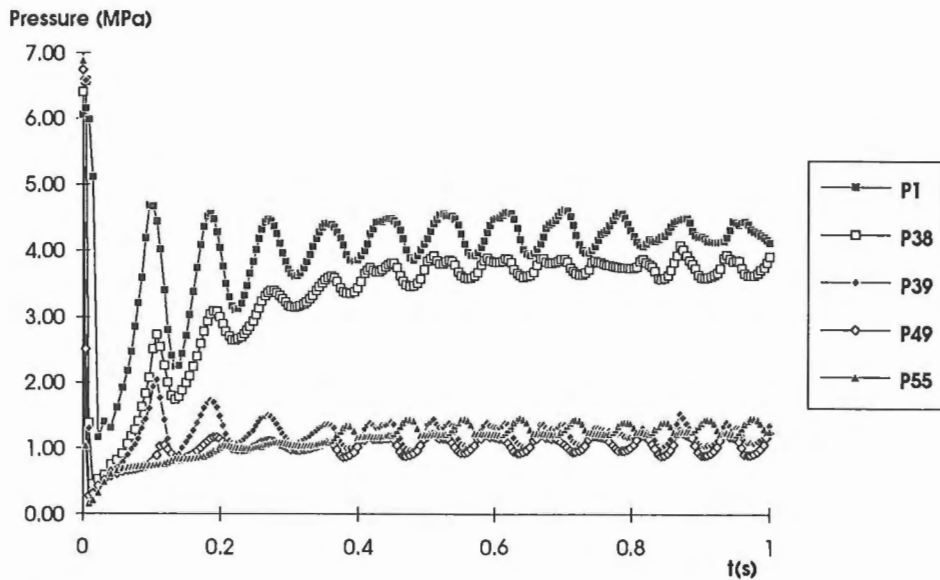
Figure 3. Equivalent pressure transients at various locations.

pressure starts to rise towards the value used as a boundary condition for the steam generator.

During the time period of interest, the flow velocities attained in the discharge line are typically 20 m/s while the jet velocity at the broken pipe end is as high as 40 m/s. The respective mass flow rates are in the range 1000 to 1300 kg/s. The computed equivalent pressures exhibit strong oscillations as the travellig pressure waves are reflected at the pipe ends and throttlings. Continuing the analysis until time 2.2 s would indicate that the oscillations fade out as soon as the warmer water contained in the remote parts of the main feed water line reaches the discharge line and increases the void fraction.

STRUCTURAL DYNAMIC ANALYSIS

The structural dynamic analysis was done using the general purpose finite element code ABAQUS /7/. The finite element model of the discharge line, including 62 pipe and elbow elements, is shown in Fig. 4. The straight pipes were modelled with elements of the type PIPE31, while both ELBOW31 and ELBOW31B type elbow elements were adopted in modelling the bends with radius of curvature 600 mm. The density of steel was modified in all pipe elements to incorporate the mass of the contained liquid water. Valves V1 and V2 of Fig. 2, each having a mass of 978 kg, were modelled with lumped masses located at nodes 15 to 17 and 19 to 21, respectively.

The ELBOW31 type elements allow cross-sectional ovalization and warping, whereas the PIPE31 type beam elements expand only radially. ELBOW31B, which was used in geometrically nonlinear analysis, is based on a simplified formulation where ovalization only is accounted for. This makes the element somewhat overly flexible, as it does not consider the inter-element compatibility of axial gradients associated with ovalization. All elbow elements used in the analyses incorporate six circumferential Fourier modes for ovalization, seven integration points through the wall thickness, one integration point in the axial direction and 18 circumferential integration points.
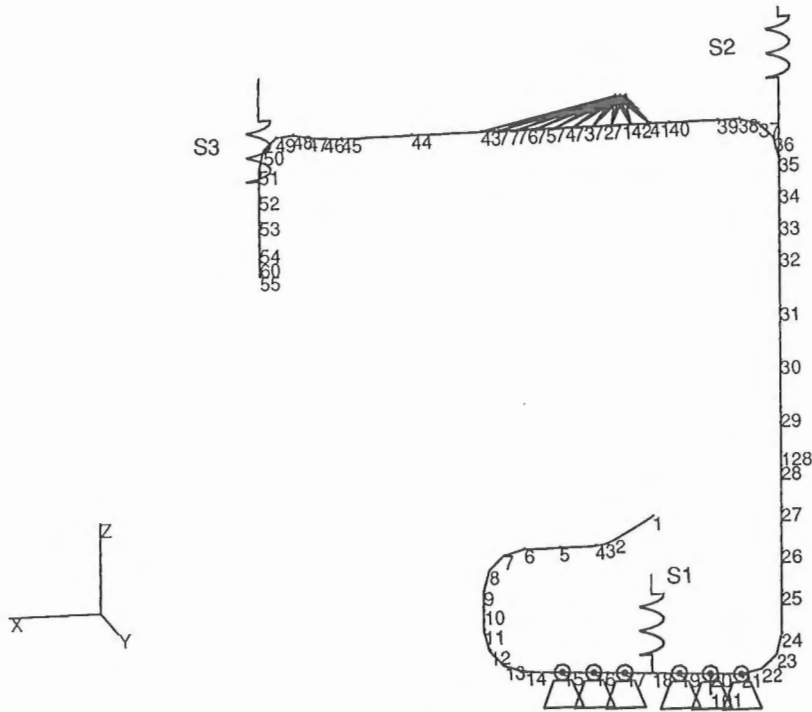
Fig. 4. Finite element model of the discharge line.

The downstream end of the model is located at the T-connection (node 1) and is treated as fully fixed. This assumption is justified by the greater rigidity of the main feed water line, which has one rigid and one sliding support near the T-connection. The discharge line is additionally supported by three spring hangers S1, S2 and S3, composed of springs and bars joined with hinges. A bilinear spring model, which carries only tension, was used in their finite element analysis. The spring constant of S1 is 630 N/mm and 440 N/mm for both S2 and S3. Whenever the deformation capacity of the springs was exceeded, the slope of the force-displacement curve of the model was taken to match the axial stiffness of the bar.

The lower flange of the horizontal I-beam, located above the topmost horizontal straight portion, was modeled by means of several cylindrical gap elements fixed to the pipe between nodes 40 and 43. The axes of the gap elements were set perpendicular to the pipe axis. Based on the design documentation, the value 250 mm was given to the

48

distance between the gap elements and the outer pipe surface. Since local crushing of the pipe was less than the wall thickness and no measurable deflection was observed in the web of the beam, it was considered reasonable to let the gap cylinder fully constrain the normal velocity component of contacting pipe. Another contact possibly occurred at a hole of diameter 700 mm, made in a concrete floor (level +3.00) for penetration of the long vertical portion of the discharge line. Some spring elements, fixed to nodes 28 and 128, were inserted along the circumference, which was assumed to be concentric with the penetrating pipe cross-section prior to the event.

An elastic-plastic material model with the von Mises yield function and isotropic strain hardening was applied in the analysis. Poisson's ratio was set to 0.3 and a piecewise linear stress-strain curve was defined by the values of Table 1. The effect of the operating temperature 165° C on the CT20 ferritic pipe material was estimated using the stress-strain curves given by a Russian standard /8/.

Table 1. True stress-strain values of the pipe material.

Strain[mm/mm]	0.0019	0.004	0.0218	0.0529	0.1824	0.29
Stress [MPa]	360.0	364.0	379.9	418.2	456.2	460.0

The strain rates during the event were of sufficient magnitude to affect the mechanism of plastic flow. A standard procedure for considering the strain rate effects is given by the formula

$$\dot{\epsilon}_{pl} = D \left[\frac{\tilde{\sigma}}{\sigma^0} - 1 \right]^p \tag{1}$$

where $\dot{\epsilon}_{pl}$ is the equivalent plastic strain rate, $\tilde{\sigma}$ is the effective yield stress and σ^0 is the static yield stress /7/. For structural steels, the material parameters D and p typically assume the values 40 and 5, respectively. Equation (1) implies an increase in

the yield strength, which is well known from experiments on austenitic stainless steels. However, fairly recent results presented by the International Piping Integrity Research Group /9/ suggest that ductile ferritic steels exhibit an opposite phenomenon, known as dynamic strain aging, which instead lowers the ultimate tensile strength at simultaneous high strain rates and temperatures; while the yield strength remains virtually unchanged. Owing to a lack of directly applicable data, results based on Equation (1) and the above material parameter values are presented parallel to those obtained with the static data of Table 1.

A Rayleigh type damping, proportional to the mass matrix, was introduced in the model to find permanent displacements by direct time integration. The proportionality factor was determined in such a manner that a damping ratio of 5% was achieved for the lowest eigenmodes which dominated elastic vibrations at the broken pipe end (node 55). Damping was speeded up by ignoring the fluid dynamic excitation after time 1 s, whereafter it was too weak to produce plastic deformation.

RESULTS

The ten lowest eigensolutions of the discharge line were first evaluated using a linearized model which disregarded the gaps and spring supports. Two sets of eigenfrequencies, corresponding to bends modelled with ELBOW31 and ELBOW31B elements, are listed in Table 2.

Table 2. Eigenfrequencies [Hz].

Mode	1.	2.	3.	4.	5.	6.	7.	8.	9.	10.
31	0.55	0.61	1.23	1.40	2.83	2.94	5.57	7.99	11.1	11.8
31B	0.56	0.61	1.25	1.42	2.87	2.98	5.78	8.15	11.2	11.9

The first mode is governed by rotation about the Y axis. The second and third modes correspond to rotations about the X and Z axes, respectively. Due to the gap and spring elements not all the vibration modes contribute to the response. At least the mode moving the discharge line in the Y direction can be identified.

Three dynamic nonlinear analyses were carried out using automatic time stepping in direct time integration. The time increments typically assumed values of ca. 10^{-3} s during the applied excitation, whereas during contacts values as small as 10^{-10} s proved necessary. The first analysis was elastic-plastic; the second was elastic-plastic including the strain rate effect; and the third accounted for both the strain rate effect and geometrical nonlinearity. These analyses, referred to as A, B and C respectively, were performed on a Silicon Graphics Crimson workstation. The CPU times and total number of increments needed are given in Table 3.

Table 3. CPU times and increments needed in the dynamic nonlinear analyses.

Analysis	A	B	C
Increments	2000	1600	1300
CPU [h]	13	10	3.6

For comparison it can be mentioned that the CPU time for a run of the TMOC code over 3.0 s was several minutes on a HP9000/735 workstation.

All displacements are presented in the global coordinate system shown in Fig. 4. The displacement components predicted by analysis A at the break point of the piping are shown in Fig. 5 as a function of time. The vibration in the Y direction is mainly caused by the second eigenmode. The maximum value of the vertical displacement (Z direction) is 1.01 m. An approximate value of 0.40 m was estimated for the vertical plastic displacement. The corresponding plastic displacement values for analyses B and C were roughly 200 and 150 mm, respectively. After the first impact against the beam

51

at time 0.27 s this vertical displacement curve descends more steeply. The pipe hits the beam several times and gives rise to a maximum contact force of a 3.0 MN. A similar result was obtained in analyses B and C.
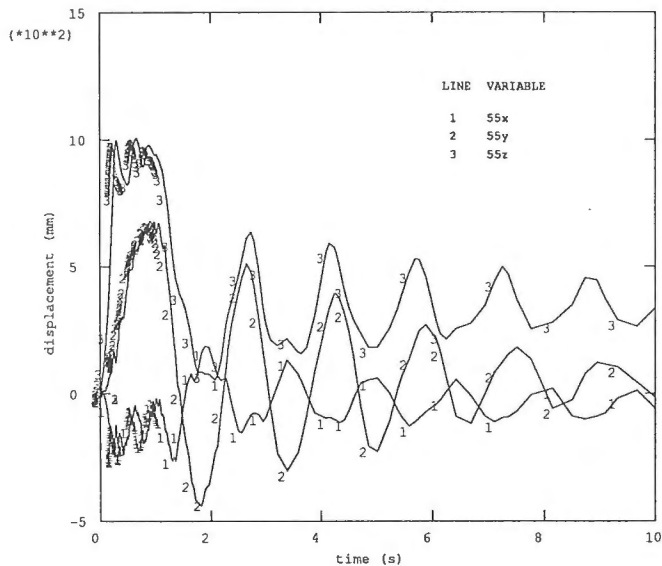
Fig. 5. Displacement components of the break point versus time.

By the time it impacts with the beam, the pipe has attained a maximum negative displacement in the X direction of nearly 0.5 m. The horizontal displacement of node 35 in the X direction is shown in Fig. 6. A maximum of 0.49 m is attained upon impact. The same result was obtained with analysis B, whereas analysis C yielded a value of 0.46 m. The piping was about to impact with a vertical wall 0.48 m away (see Fig. 2). However, no impact marks were detected. A similar conclusion applies to the downward vertical displacement of node 21, also seen in Fig. 5, since values exceeding 275 mm would have caused the valves to impact with a nearby floor.

According to the geometrically linear analyses A and B, the vertical part of the piping touched the wall at the penetration. The radial displacement at the penetration, also shown in Fig. 6, is roughly 190 mm at the most, which equals the distance between the wall and the outer surface of the pipe. However, no evidence of impact was observed.
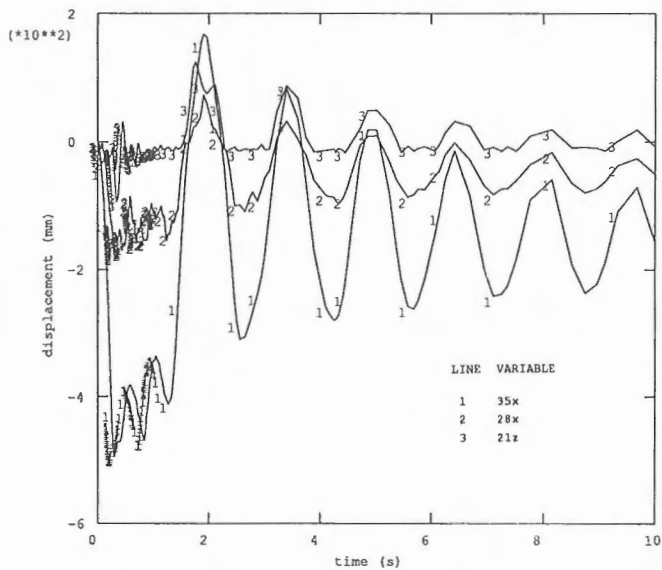
Figure 6. Displacement components of nodes 21, 28 and 35 versus time.

Each analysis predicted plastic deformation at the bends and pipe portions which impacted with the beam. The plasticity due to the impact would have a pronounced effect on the vertical displacements of the break point. As the degree of plasticity in turn was particularly sensitive to the strain rate effect, it is evident that analysis A, based on static stress-strain data, would produce the highest permanent displacements of the break point. Underestimation of the measured value by some 30%, even in analysis A, may be attributed mainly to the following factors: 1) uncertainty of the static stress-strain curve; 2) effect of dynamic strain aging on strain hardening; 3) contact phenomena during impacts against the beam; 4) thermal hydraulic assumptions affecting the excitation. These aspects clearly deserve further investigation. However, owing to the significant flexibility of the discharge line during upward motion, the instantaneous maximum displacements probably would have compared much better. This quantity actually governs the effect of pipe whip on plant safety; hence reasonable accuracy is expected in licencing applications.

CONCLUSION

The results of this study indicate that existing general purpose thermal hydraulic and elastic-plastic finite element codes are powerful tools for making extensive and realistic pipe whip analyses. The thermal hydraulic analysis was fairly straight-forward, although some uncertainties emerged regarding the boundary conditions and physical modelling. These included the opening time of the break, the formation rate of steam bubbles, and the way of modelling the pipe network beyond the T-connection. However, the results are felt to be reliable over the significant time period of fluid dynamic excitation. Similar conclusions apply to the finite element analysis, which was strongly affected by the applied stress-strain curve and assumptions regarding impacts against nearby structures. Contact-dynamic formulation and material-specific data on strain-rate effects at the operating temperature would certainly improve the results. The experimental data from the real pipe break event analysed in this study were too scant to allow benchmarking of the applied analysis procedures, but indicate that reasonable accuracy may be expected in licencing analyses and other practical applications.

ACKNOWLEDGEMENTS

REFERENCES

/1/ Beaudoin, B. F., Quinones, D. F. and Hardin, T. C. Leak-Before-Break Application in US Light Water Reactor Balance-of-Plant Piping. Int. J. of Pressure Vessels and Piping, Vol. 43, Nos 1-3, 1990, pp. 67-83.

/2/ Lazzeri, L., Pipe Whip Analysis. Advanced Structural Dynamics. Edited by J. Donea. Applied Science Publishers Ltd, London, 1978, pp. 387-426.

/3/ NEA-IRS NO. 1352.02. Organization for Economic Cooperation and Development, Nuclear Enegy Agency. Incident Reporting System 1993.

/4/ Siikonen, T., A Short Description of the Computer Code TMOC. VTT Resarch Notes 257, Espoo 1983, 70 p. + app. 23p.

/5/ Siikonen, T., Computational Model for the Analysis of Valve Transients, J. of Pressure Vessel Technology, Vol. 105, No. 3, Aug. 1983, pp. 227-233.

/6/ Keskinen, R., Hydroelastic Piping Vibration Analysis by Transfer Matrices. Int. J. of Pressure Vessels and Piping, Vol. 9, 1981, pp. 263-283.

/7/ ABAQUS User & Theory Manuals (1992) Hibbit, Karlsson & Sörensen, Version 5.2.

/8/ Strength Calculation Standards for Components and Pipelines of Nuclear Power Plants. PNAEG-7-002 86. Moscow. Energoatomizdat 1989.

/9/ Brickstad, B., An evaluation of the IPIRG program (In Swedish). SA/FoU-Rapport 91/5. The Swedish Plant Inspectorate. Stockholm 1991.

Arja Saarenheimo, VTT/Manufacturing Technology
Lauri Eerikäinen, VTT/Energy
Rauli Keskinen, Finnish Centre for Radiation and Nuclear Safety